

Short Communications

Synthesis of Rodlike CaTiO₃ with Enhanced Charge Separation Efficiency and High Photocatalytic Activity

Xin Yan¹, Xiaojun Huang¹, Ying Fang¹, Yahong Min¹, Zhenjun Wu^{1,*}, Wensheng Li¹, Jianmin Yuan², Ligang Tan³

¹College of Chemistry and Chemical Engineering, Hunan University, Changsha, 410082, P. R. China

²College of Materials Engineering, Hunan University, Changsha, Hunan 410082, P. R. China

³College of Mechanical and Vehicle Engineering, Hunan University, Changsha, Hunan 410082, P. R. China

*E-mail: wooawt@163.com

Received: 29 April 2014 / Accepted: 17 May 2014 / Published: 16 June 2014

Rodlike CaTiO₃ was prepared by a simple thermal method. The as-prepared samples presented relatively enhanced photo induced charge separation and high photocatalytic activity toward methyl orange in aqueous solution. The band gap of the CaTiO₃ with special morphology was narrowed. The photoreactivity observed on CaTiO₃ was attributed to the large amount of active sites, great oxidation potential of photogenerated holes and high separation efficiency of photogenerated electrons and holes.

Keywords: CaTiO₃; Photocatalysis; Rodlike; Charge separation

1. INTRODUCTION

The widespread disposal of industrial wastewater containing organic dyes has led to serious contamination in many countries worldwide [1]. These organic dyes, particularly azo dyes [2], are readily reduced to potentially hazardous aromatic amines, which impart adverse effects on animal and human health. Therefore, the removal of organic pollutants in wastewater is a huge task in environmental protection. Amongst various measures [3-5], photosensitized degradation on titanium dioxide has proven to be the most widely used, owing to its low cost, non-toxicity, chemical stability and long-term photostability [6, 7]. When illuminated with an appropriate light source, the free electrons are excited to the empty conduction band and leave positive holes in the valence band, resulting in the formation of electron-hole pairs on the photocatalyst. The holes are trapped by water (H₂O) or hydroxyl groups (OH⁻) adsorbed on the surface to generate hydroxyl radicals (OH[•]), which is a powerful oxidizing agent for mineralizing the pollutants [8-13]. Substantially, the

photocatalytic efficiency of many catalysts which degrade dyes decreases because of the wide holes produced when irradiated under ultraviolet light and consequently causes disastrous structural damage [14-16]. Thus, developing new photocatalytic materials entailing optical band gap, carrier transport, catalytic activity surface properties and chemical stability is a challenging endeavor [17].

Due to the wide band gap (3.5 eV), CaTiO_3 was rarely used for the photodegradation of organic dyes. However, as a perovskite composite, it has many unique structural features [18], including the defined structure, the variable composition, and so on. The defined structure makes it possible to introduce various metal ions in its structure framework and the Ca^{2+} and Ti^{4+} can be substituted by a foreign one without destroying the matrix structure, which allows controlled alternation of the oxidation state of cations or changing the intrinsic band structure of CaTiO_3 . Consequently, it improves the light sensitivity [19] as well as increases the photocatalytic activity.

In this paper, rodlike CaTiO_3 was synthesized by a method referred to the work of Zhao et al [20] without the electrospinning process. In this way, the process become energy saving and could be widely used in the preparation of special materials as the process was simplified. Recently, CaTiO_3 has received much attention as a promising material for photoelectrochemical water-splitting because it has a similar band structure to TiO_2 , and matches the energy levels of water splitting [21]. The special like CaTiO_3 was rarely synthesized and applied in photodegradation of organic dyes. We compared the electrochemical and photocatalytic performance of the CaTiO_3 with the special morphology to the CaTiO_3 with traditional morphology. The as-prepared samples showed narrowed band gap and relatively enhanced photo induced charge separation, which resulted in the high photocatalytic activity for the photodegradation of methyl orange in aqueous solution under the irradiation of simulated solar light.

2. EXPERIMENTAL SECTION

2.1. Materials preparation

All reagents used in this research were analytical grade and used without further purification. Distilled water was used in all experiments. The typical preparation of rodlike CaTiO_3 was as follows. Firstly, 0.45 g of polyvinyl pyrrolidone was added into 3 ml of ethanol then the mixture was stirred for 2 h to make the polyvinyl pyrrolidone totally dissolved. Secondly, 0.05 mol of $\text{Ca}(\text{NO}_3)_2$ and tetra-n-butyl titanate were dissolved in ethanol, respectively. Thirdly, the $\text{Ca}(\text{NO}_3)_2$ solution was dropwise added to the polyvinyl pyrrolidone solution, followed by the acidification by acetic acid and the tetra-n-butyl titanate solution was added afterward. The transparent and vicious mixture was stirred for 10 h, then slowly vaporized at 60 °C and opaque powder was obtained. Finally, the powder was calcined at 700 °C for 5 h in air, and the rodlike CaTiO_3 was obtained. By contrast, grainy CaTiO_3 was prepared by coprecipitation method which adopted ammonium oxalate as the precipitant.

To investigate the photoelectrochemical performance of the sample, the electrodes were prepared as follows, 5 mg of sample and 3 mg of polyethylene glycol 6000 (PEG-6000) was suspended in 3 ml of ethanol to produce slurry, which was then dip-coated onto a ITO (indium tin oxide) glass

substrates (3 cm × 2 cm) with a sheet resistance of 15 Ω. After being dried, the as-prepared electrodes were calcinated at 400 °C for 0.5 h to remove the PEG-6000.

2.2. Characterization

The crystal phases of the samples were determined by an X-ray diffractometer with Cu-Kα radiation (XRD, Rigaku D/Max 2500). Diffusion reflection spectra (DRS) collection was carried out on a Cary 300 UV-Vis spectrophotometer with an integrating sphere using BaSO₄ as the reference sample. The morphology of the samples was detected by scanning electron microscope (SEM, Hitachi S4800). The photoelectrochemical experiment was carried out on an electrochemical system (CHI-D66H, China).

2.3. Photocatalytic Experiments

The photocatalytic activities were evaluated by the decomposition of methyl orange under a 500 W xenon lamp. A aqueous suspension of methyl orange (50 ml, 10 mg L⁻¹) was placed in a quartz beaker and 15 mg of photocatalysts was added. Prior to irradiation, the suspensions were ultrasonicated for 10 min and magnetically stirred in the dark for 30 min to reach the absorption-desorption equilibrium. At given intervals, 0.5 ml of the aliquots were sampled and analyzed by recording variations in the absorption band (465 nm) in the UV-visible spectra of methyl orange using a Cary 300 spectrophotometer.

2.4 Photoelectrochemical Measurements

Photoelectrochemical tests were carried out in a conventional three-electrode single-compartment quartz cell filled with 0.1 M Na₂SO₄ electrolyte, using a potentiostat. The ITO/ CaTiO₃ electrode served as the working electrode, the counter and reference electrodes were a platinum black and a saturated calomel electrode (SCE), respectively. A 500 W xenon arc lamp with the photon flux of 100 mW cm⁻² (CHF-XQ-500W, Beijing Changtuo Co.Ltd) with a bias of 0 V (vs SCE) was used as the excitation light source.

3. RESULTS AND DISCUSSION

3.1. Structure and Optical Properties

Fig. 1 shows the SEM images of CaTiO₃ with different morphologies prepared by different methods. The surface of rodlike CaTiO₃ (Fig. 1 a) is coarse with many particles adhering to it. The grainy CaTiO₃ (Fig. 1 b) with uniform size stack together in an irregular pattern, forming the porous structure. XRD analysis (Fig. 2) shows that all the diffraction peaks of both as-prepared samples are

in good agreement with those of the structure of CaTiO_3 (JCPDS file No. 42-0423) and the peak shape of rodlike CaTiO_3 (Fig. 2 a) is sharper, indicating its higher crystallinity. Takeshi Kimijima et al [22] had proved that the rodlike CaTiO_3 showed higher activity than cubic particles for H_2 evolution because of the preferential production of photoexcited electrons. However, the band gap of the as-prepared rodlike particles was about 3.63 eV indicating higher energy needed for exciting electrons from valence band to conductive band. The rodlike CaTiO_3 that we have prepared is different from Takeshi Kimijima's work in morphology and thus results in the different band gap. The UV-Vis diffuse reflectance spectra of CaTiO_3 are shown in Fig. 3. The absorption spectra of two morphologies are almost the same, and the grainy CaTiO_3 has a weak absorption in the visible light region. The direct optical band gap from the absorption spectra for CaTiO_3 is shown in the inset of Fig. 3a and Fig 3b. An optical band gap is obtained by plotting $(\alpha h\nu)^2$ versus $h\nu$, where α is the absorption co-efficient and $h\nu$ is photon energy. Extrapolation of the linear portion at $(\alpha h\nu)^2 = 0$ gives the band gap of 3.08 eV for the rodlike CaTiO_3 and 3.28 eV for the grainy CaTiO_3 . Thus, for the rodlike CaTiO_3 , the minimum energy required for the excitation of an electron from valence to conduction band is lower than the grainy CaTiO_3 .

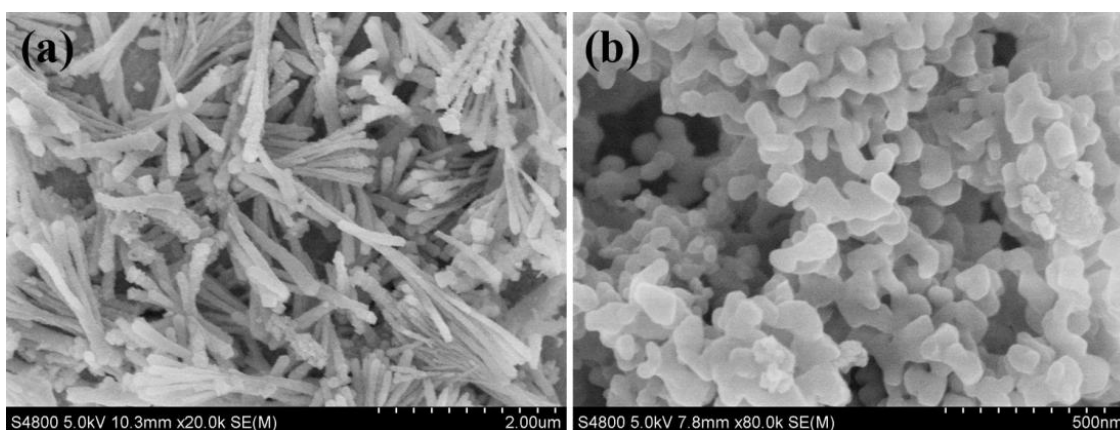


Figure 1. SEM images of the rodlike CaTiO_3 (a) and the grainy CaTiO_3 (b)

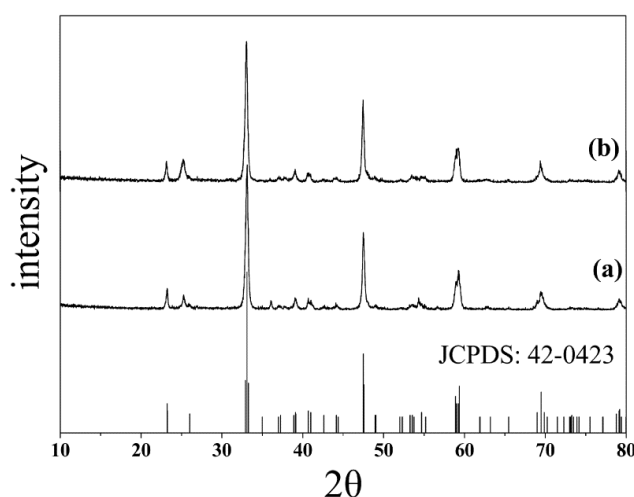


Figure 2. XRD patterns of the rodlike CaTiO_3 (a) and the grainy CaTiO_3 (b)

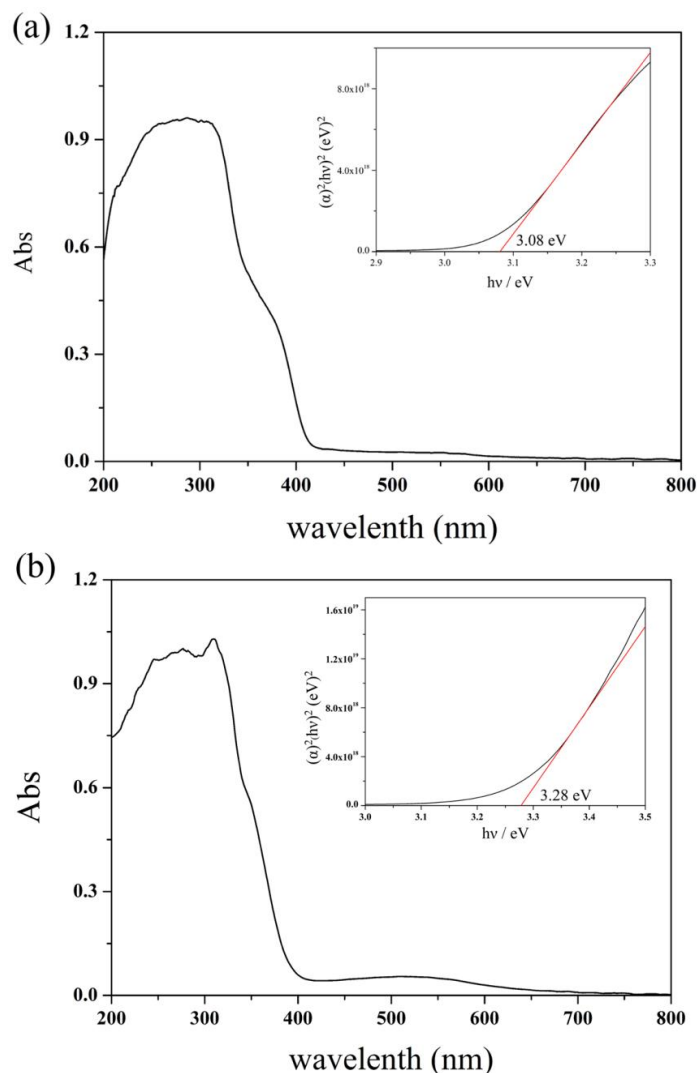


Figure 3. UV-Vis diffuse reflectance spectra of rodlike CaTiO₃ (a) and grainy CaTiO₃ (b). The inset shows the estimated band gap of samples

3.2 Enhancement of Photoelectrochemical Activity

The photogenerated charge separation efficiency could be investigated by the photocurrent spectra under irradiation of simulated solar light. As shown in Fig. 4, the photocurrent density of the rodlike CaTiO₃ electrode is about twice as high as that of the grainy CaTiO₃ electrode. Moreover, the photocurrent density of the rodlike CaTiO₃ electrode is steady while the other weakens gradually as time went on. This clearly indicates that the rodlike morphology improves the separation efficiency of photoinduced electrons and holes. It is generally believed that the recombination of photoexcited electrons and holes is one of the most detrimental factors negatively impacting the photocatalytic activity, and that lattice defects work as the recombination center [23]. Therefore, there are less lattice defects for the photoinduced charge recombination in the rodlike CaTiO₃. The photoresponsive phenomenon might be one of the reasons for the enhanced photocatalytic activity.

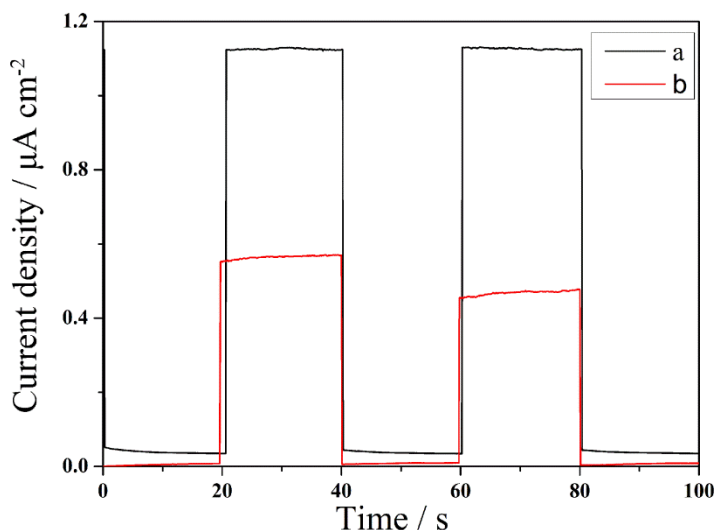


Figure 4. The photoresponses of rodlike CaTiO_3 (a) and grainy CaTiO_3 (b)

3.3. Enhancement of Photocatalytic Activity

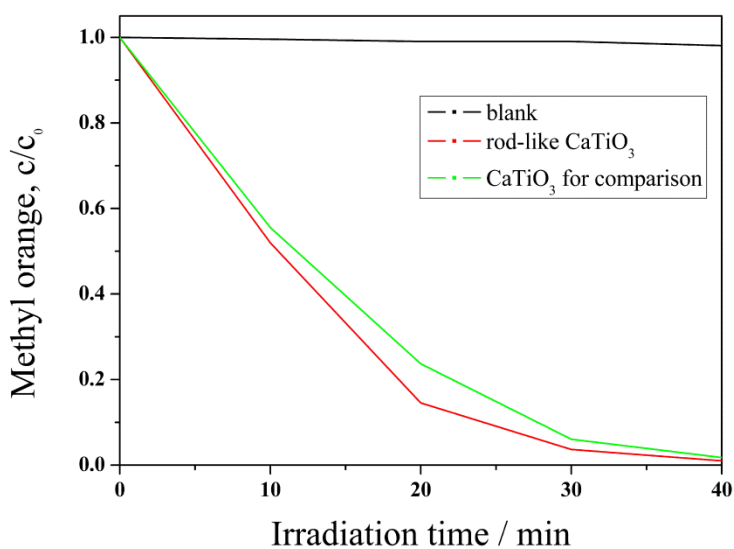


Figure 5. Comparison of photocatalytic activity of rodlike CaTiO_3 and grainy CaTiO_3

The photodegradation of methyl orange under the irradiation of simulated solar light was carried out to investigate the performance of photocatalysts. The degradation process was also implemented without any photocatalysts under the same light for comparison. The grainy CaTiO_3 was used as the reference photocatalysts. Seen in Fig. 5, the blank test confirmed that the methyl orange was slightly degraded in the absence of catalysts, indicating that the photolysis could be ignored. Both the rodlike CaTiO_3 and grainy CaTiO_3 exhibited high activity towards the degradation of methyl orange. However, the rodlike photocatalysts shows higher activity that can degrade 10 mg L^{-1} methyl

orange by 99.03% while the grainy CaTiO_3 can degrade 98.15% in 40 min when the concentration of the catalyst is 0.3 g L^{-1} . Assuming that the photocatalytic reaction follows a pseudo-first-order reaction, the rate constant of methyl orange decomposition by rodlike CaTiO_3 is estimated to be about 0.116, faster than that of grainy CaTiO_3 which is estimated to be about 0.0982. It reveals that CaTiO_3 has good photodegradation effect to methyl orange and the rodlike CaTiO_3 is better than the grainy CaTiO_3 . This may attribute to narrower band gap, the coarse surface and the higher photoinduced charge separation efficiency of the rodlike CaTiO_3 [24-27]. Due to the narrower band gap, it is easier for the electrons to be excited from the valence band to the conductive band, which result in the higher production efficiency of electron-hole pairs. The coarse surface provides bigger surface area for absorbing photons with appropriate energy and more active sites for the degradation process. The enhanced quantum efficiency ensures the valid and high degradation rate of methyl orange.

3.4 Proposed Photocatalytic Mechanism

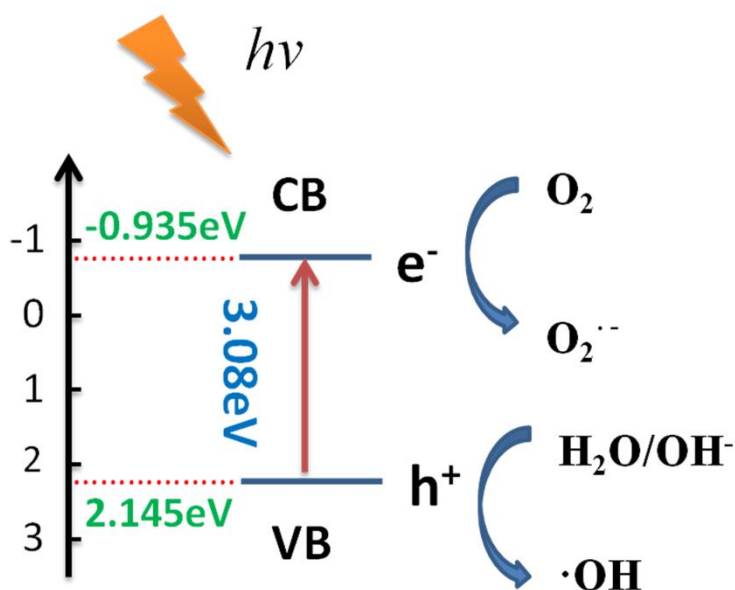


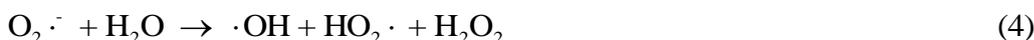
Figure 7. Diagram for band energy of rodlike CaTiO_3 and chart of photocatalytic mechanism

In general, the photocatalytic activity is determined by the band gap, the oxidation potential of photogenerated holes and the separation efficiency of photogenerated electrons and holes [21]. To investigate the oxidation potential of photogenerated holes, the conduction band (CB) and valence band (VB) potentials of CaTiO_3 at the point of zero charge can be calculated by the following equation [22, 23]

$$E_{\text{VB}} = X - E_{\text{c}} + 0.5E_{\text{g}} \quad (1)$$

Where X is the absolute electronegativity of the semiconductor, which is defined as the geometric mean of the absolute electronegativity of the constituent atoms, E^{c} is the energy of free electrons on the hydrogen scale (ca. 4.5 eV), E_{VB} is the VB edge potential, and E_{g} is the band gap of the semiconductor.

The conduction band (CB) position can be calculated by $E_{CB} = E_{VB} - E_g$. The X value for CaTiO_3 is 5.105. According to the above equations, the top of the CB and the bottom of the VB of CaTiO_3 are -0.935 eV and 2.145 eV, respectively. The results indicate that the oxidation potential of photogenerated holes is high, resulting in the high photoactivity of CaTiO_3 . On the basis of the above results, we proposed the following mechanism (shown in Fig. 6). When CaTiO_3 was irradiated by the simulated solar light, the electrons of CaTiO_3 were excited from the valence band (VB) to the conduction band (CB). Then the photoinduced electrons of the CB could be transferred to the dissolved oxygen to form superoxide anion radicals ($\text{O}_2^{\cdot-}$), which subsequently transform to active oxygen species, such as HO_2^{\cdot} , $\cdot\text{OH}$ and H_2O_2 due to the higher potential of CB (-0.197 eV) than that of $\text{O}_2 / \text{HO}_2^{\cdot}$ (-0.046 eV) and $\text{O}_2 / \text{H}_2\text{O}_2$ (0.68 eV). On the other hand, the remaining holes at the valence band of CaTiO_3 reacted with adsorbed water or surface hydroxyl groups (OH^{\ominus}) to produce $\cdot\text{OH}$ radicals [24]. These $\cdot\text{OH}$ radicals and the holes were responsible for the degradation of methyl orange. The major initial steps in the mechanism under irradiation are summarized by Eqs. (2) - (6)



4. CONCLUSION

In summary, we synthesized the rodlike CaTiO_3 by a simple thermal method. The rodlike CaTiO_3 showed the narrower band gap and increased photocurrent density, which resulted in the lower excitation energy and the high separation efficiency of photoinduced charge. The coarse surface of rodlike CaTiO_3 , the narrowed band gap and the high separation efficiency of photoinduced electrons and holes were the reasons for the enhanced photocatalytic activity.

ACKNOWLEDGEMENTS

We gratefully thank the National Natural Science Foundation of China (NSFC, Project No. 50702020 and 81171461), Natural Science Foundation of Hunan (NSFH, Project No. 11JJ4013) and Provincial Science & Technology Project of Hunan (Project No. 2013GK3155) for financial support.

References

1. F. Fu, W. Han, B. Tang, M. Hu and Z. Cheng, *Chem. Eng. J.*, 232 (2013) 534.
2. W.-S. Kuo and W.-Y. Chen, *Int. J. Photoenergy*, 2012 (2012)
3. J. Wang, Y. Guo, B. Liu, X. Jin, L. Liu, R. Xu, Y. Kong and B. Wang, *Ultrason. Sonochem.*, 18 (2011) 177.
4. R. Xu, J. Li, J. Wang, X. Wang, B. Liu, B. Wang, X. Luan and X. Zhang, *Sol. Energy Mater. Sol. Cells*, 94 (2010) 1157.

5. W. Zhang, H. L. Tay, S. S. Lim, Y. Wang, Z. Zhong and R. Xu, *Appl. Catal. B.*, 95 (2010) 93.
6. K. Pirkanniemi and M. Sillanpää, *Chemosphere*, 48 (2002) 1047.
7. X. Chang, J. Huang, C. Cheng, Q. Sui, W. Sha, G. Ji, S. Deng and G. Yu, *Catal. Commun.*, 11 (2010) 460.
8. S. Sakthivel, B. Neppolian, M. Shankar, B. Arabindoo, M. Palanichamy and V. Murugesan, *Sol. Energy Mater. Sol. Cells*, 77 (2003) 65.
9. O. Akhavan, *J. Colloid Interface Sci.*, 336 (2009) 117.
10. J. Robertson, P. K. J Robertson and L. A. Lawton, *J. Photochem. Photobio A.*, 175 (2005) 51.
11. V. Nadtochenko, A. Rincon, S. Stanca and J. Kiwi, *J. Photochem. Photobio A.*, 169 (2005) 131.
12. P. Bouras and P. Lianos, *Catal. Lett.*, 123 (2008) 220.
13. U. Akpan and B. Hameed, *J. Hazard. Mater.*, 170 (2009) 520.
14. H. Zhang and Y. Zhu, *J. Phys. Chem. C.*, 114 (2010) 5822.
15. H. Zhang, R. Zong and Y. Zhu, *J. Phys. Chem. C.*, 113 (2009) 4605.
16. H. Zhang, R. Zong, J. Zhao and Y. Zhu, *Environ. Sci. & Technol.*, 42 (2008) 3803.
17. H. W. Eng, P. W. Barnes, B. M. Auer and P. M. Woodward, *J. Solid State Chem.*, 175 (2003) 94.
18. J. Zhu and A. Thomass, *Appl. Catal. B.*, 92 (2009) 225.
19. J. C. Yu, W. Ho, J. Yu, H. Yip, P. K. Wong and J. Zhao, *Environ. Sci. & Technol.*, 39 (2005) 1175.
20. G. Gong, J. Wu, J. Liu, N. Sun, Y. Zhao and L. Jiang, *J. Mater. Chem.*, 22 (2012) 8257.
21. H. Zhang, G. Chen, X. He and J. Xu, *Mater. Res. Bull.*, 47 (2012) 4483.
22. T. Kimijima, K. Kanie, M. Nakaya and A. Muramatsu, *Cryst. Eng. Comm.*, (2014)
23. T. K. Ghorai and N. Biswas, *J. Mater. Res. Technol.*, 2 (2013) 10.
24. F. Meng, Z. Hong, J. Arndt, M. Li, M. Zhi, F. Yang and N. Wu, *Nano Res.*, 5 (2012) 213.
25. W. Wang, B. Huang, X. Ma, Z. Wang, X. Qin, X. Zhang, Y. Dai and M. H. Whangbo, *Chem-A. Euro. J.*, 19 (2013) 14777.
26. T. Xu, L. Zhang, H. Cheng and Y. Zhu, *Appl. Catal. B.*, 101 (2011) 382.
27. K. Zhang, D. Kopetzki, P. H. Seeberger, M. Antonietti and F. Vilela, *Angew. Chem.*, 125 (2013) 1472.
28. Q. Xiang, J. Yu and M. Jaroniecs, *J. Am. Chem. Soc.*, 134 (2012) 6575.
29. G. Dai, J. Yu and G. Liu, *J. Phys. Chem. C.*, 116 (2012) 15519.
30. Y. Xu and M. A. Schoonens, *Am. Mineral.*, 85 (2000) 543.
31. X. Liu, Y. Tang, S. Luo, Y. Wang, X. Zhang, Y. Chen and C. Liu, *J. Photochem. Photobio. A.*, (2013)22.